PGE 383 Project Update #5 - Team 01

Preston Fussee-Durham, Ningjie Hu, Jayaram Hariharan, Jorge Navas

1 Executive Summary

The Reservoir Subsurface Team 1 has continued with the spatial estimation of this reservoir through simulation. This update includes efforts taken to simulate the continuity of the field for parameters of interest (porosity and permeability), and simulate the categorical variables such as facies, using techniques which are designed to preserve the structure and continuity of the field.

The indicator variograms and kriging spatial continuity for facies distributions from previous updates are applied to perform sequential indicator simulation and estimate facies locations in the field. Spatial continuity variogram models and kriging methods from the previous updates are leveraged to perform sequential gaussian simluation for porosity and permeability data on a by-facies basis. We find that the trend modeling applied was slightly overaggressive and by overfitting the data led to simulations which tend to be overly smooth and more continuous than the original data. We acknowledge this shortcoming and intend to revise it in the future updates. However we believe these simulation results (Fig. 6) are still informative and largely conform with the initial acoustic impedance data collected over the reservoir (Fig. 7). The findings in this update have led us to challenge our initial depositional setting interpretation. Previously we believed this to be a meandering channel system, however after performing these simulations, we are more receptive to the possibility of the reservoir being comprised of sandy lobes.

2 Description of Workflows and Methods

The following steps were carried out in a Jupyter Notebook workflow:

1. Using the well data and previously constructed facies indicator variogram models, sequential indicator simulation was performed to simulate different realizations of facies distributions
2. Convolution using a gaussian kernel was used to identify and remove the trends found in the sandstone and shale porosity data
3. Variogram models were fit to the porosity residuals
4. Using the simple kriging estimator, sequential gaussian simulation was conducted for porosity values by-facies
5. Data histograms, CDFs and Variograms were computed for the simulated fields and compared to the original data

6. Using the simulated porosity fields, correlation between porosity and permeability from the welldata, and the permeability variogram models from previous updates, colocated cokriging was performed to estimate the permeability fields by-facies

7. Histograms, CDFs and Variograms were computed for the simulated permeability fields and compared to the original well data

8. The sequential indicator simulated facies information was combined with the by-facies porosity and permeability simulations to combine the facies into single cookie-cutter estimate maps

3 Results

3.1 Sequential Indicator Simulation of Facies

Using the indicator variogram models for the spatial continuity in the distribution of facies throughout the reservoir, sequential indicator simulation was applied to generate maps of facies locations. The proportions of facies present in the initial data were applied to the simulation. Figure 1, displays two examples of the sequential indicator simulation results; this simulation was performed 20 times. The various simulations honor the initial data and provide reasonable simulations that seem plausible to the eye. In addition, the resulting plots are aligned with the initial interpretation and results from the previous updates.

Examples of Simulated Facies Maps

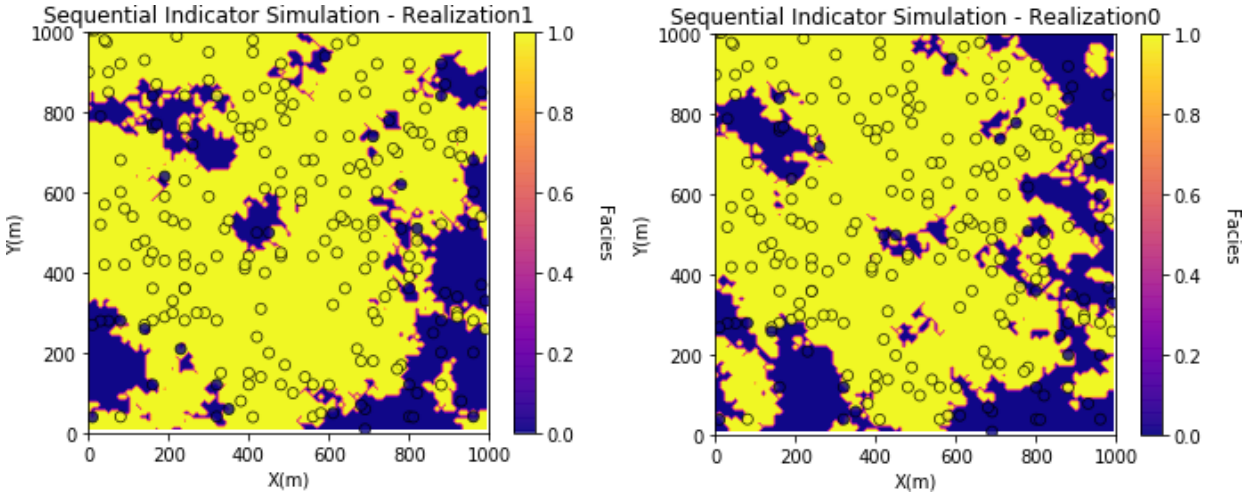

Figure 1: Facies Sequential Indicator Simulation - Sandstone shown as yellow, Shale shown as blue

3.2 Sequential Gaussian Simulation of Porosity

After using convolution with a gaussian kernel to identify and remove trends in the porosity data (by-facies), the simple kriging estimator was applied to perform sequential gaussian simulation of the porosity data. We note there is significantly more well data available in the sandstone facies (∼150 wells) compared to the shale facies (∼50 wells) making the trend and spatial continuity estimates for

properties in shale less confident than those made in sandstone. As a consequence, a broad kernel was applied for the shale trend estimation, resulting in a trend model that only fit about 10% of the variance present in the data. We were slightly more confident in the sandstone trend modeling due to the presence of more data points, and fit a tighter kernel to model about 34% of the variance with a trend.

A pair of examples of the porosity field estimates from sequential gaussian simulation for sandstone and shale are provided in Figure 2. This simulation was performed 20 times for each facies. Comparisons of the porosity CDFs for the simulated fields in comparison to the original well data are shown in Figure 3, only some realizations are plotted for clarity. We note that the CDF plots suggest that the simulations overestimate the porosity values and miss some of the behavior in the left tail, some effort needs to be taken to improve the ability of the simulations to honor the original data. The variograms of the simulated fields were computed as well, and compared to the variograms modeled using the well data. These plots were omitted from the report for brevity but we note that the tail values of the porosity we failed to simulate as seen in the CDFs, creates artificial continuity in the simulated fields that is greater than what we had previously modeled. We suspect that these misrepresentations of the data in the simulation are due to overfitting in the trend model; moving forward we plan to reconstruct more conservative trend models to create simulations that better honor the data.

Examples of Simulated Porosity Maps

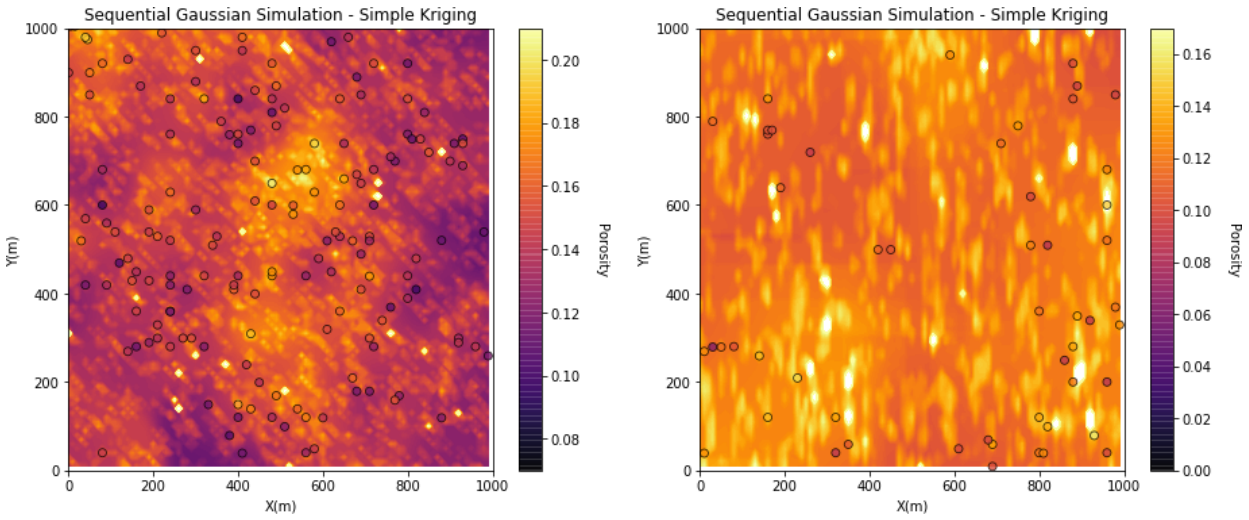

Figure 2: Simulated porosity fields - Sandstone on left, Shale on right

Cumulative Distributions of Simulated Porosity and Well Data

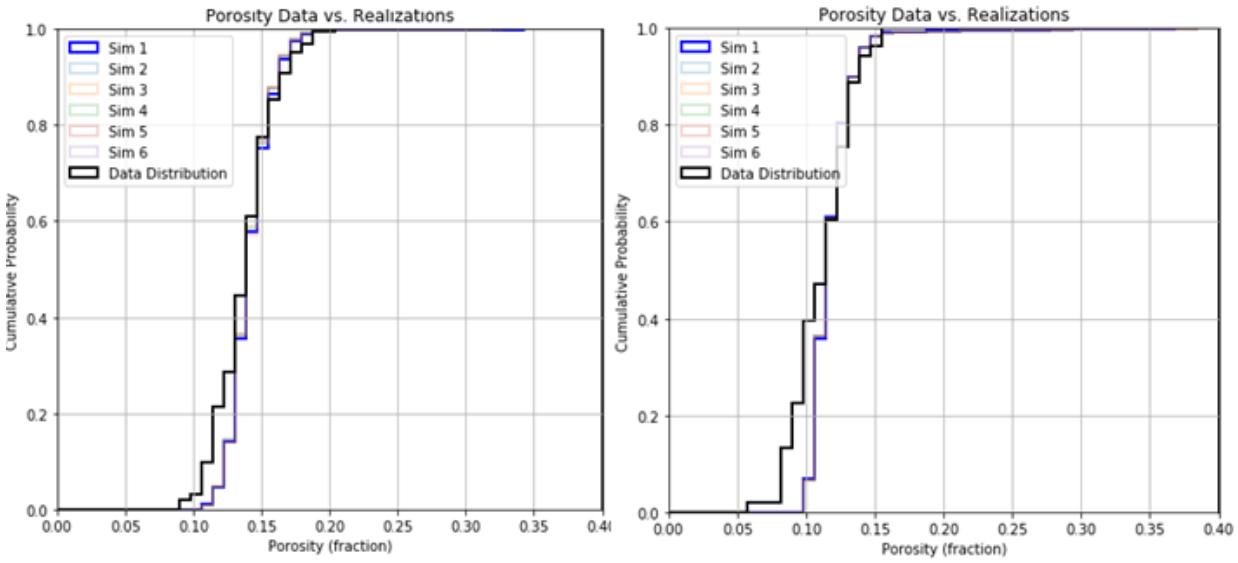

Figure 3: CDF plots of the simulated data compared to the original well data (Sandstone on left, Shale on right)

3.3 Collocated Cokriging of Permeability

Using the correlation present between the porosity and permeability in the well data (about 0.35 in sandstone and 0.2 in shale), collocated cokriging was performed to simulate 20 realizations the permeability fields. Examples of these simulated fields for both the sandstone and shale facies are shown in Figure 4. The permeability CDFs are computed for the simulated fields and compared to the original well data in Figure 5. We note that like the porosity simulations, these simulations appear to misrepresent the tails of the distributions and are more confident in their predictions of the mean permeability values than the data suggests. This mischaracterization of the distribution does lead to simulated variograms with longer ranges than the well data suggested. In future updates we plan to model the trends once more to ensure that the simulations more accurately reproduce the histograms and variograms, at this time we suspect the trends have been overfit.

Examples of Simulated Permeability Maps

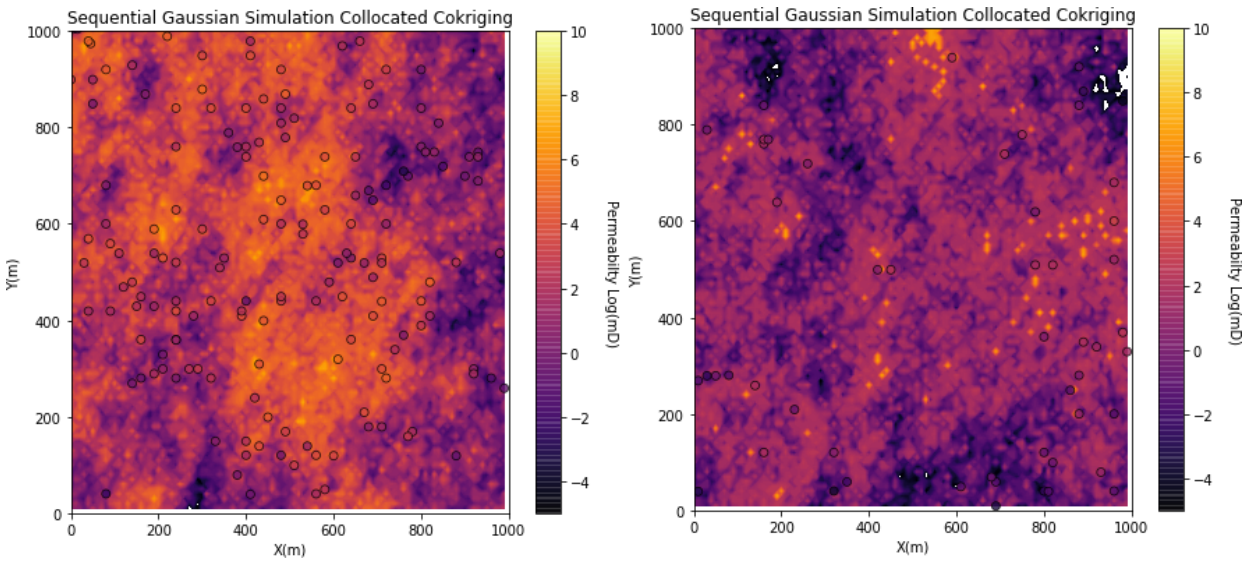

Figure 4: Simulated permeability fields - Sandstone on left, Shale on right

Cumulative Distributions of Simulated Log(mD) and Well Data

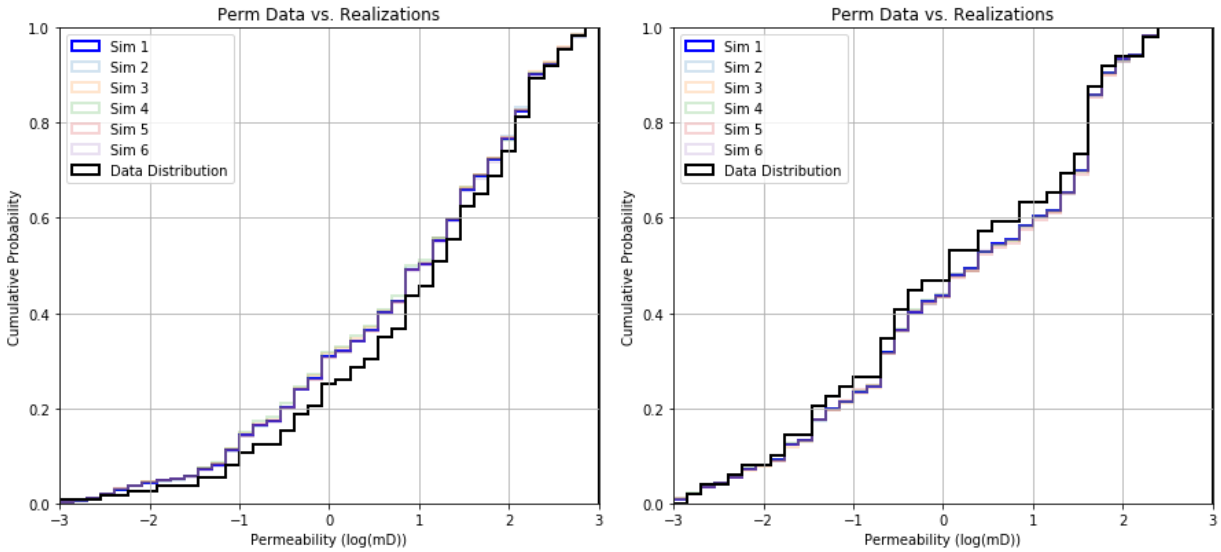

Figure 5: CDF plots of the simulated data compared to the original well data (Sandstone on left, Shale on right)

3.4 Cookie-Cutter Porosity and Permeability Maps

Using the results from the sequential indicator simulation which simulate the location of the two facies across the field, the cookie-cutter approach is applied to the simulated data. The correlation used between the porosity and permeability data was derived from the initial well data. For the shale, the correlation between porosity and permeability was about 20%, whereas for the sandstone it was about 37%. This process is repeated for the various replicates, as an example, Figure 6, is provided to show

the final results when the simulated porosity and permeability fields for each facies are combined using the sequential indicator simulation results. These results support the initial data and the locations of high permeability match the original interpretations.

Example Cookie-Cutter Fields of Porosity and Permeability

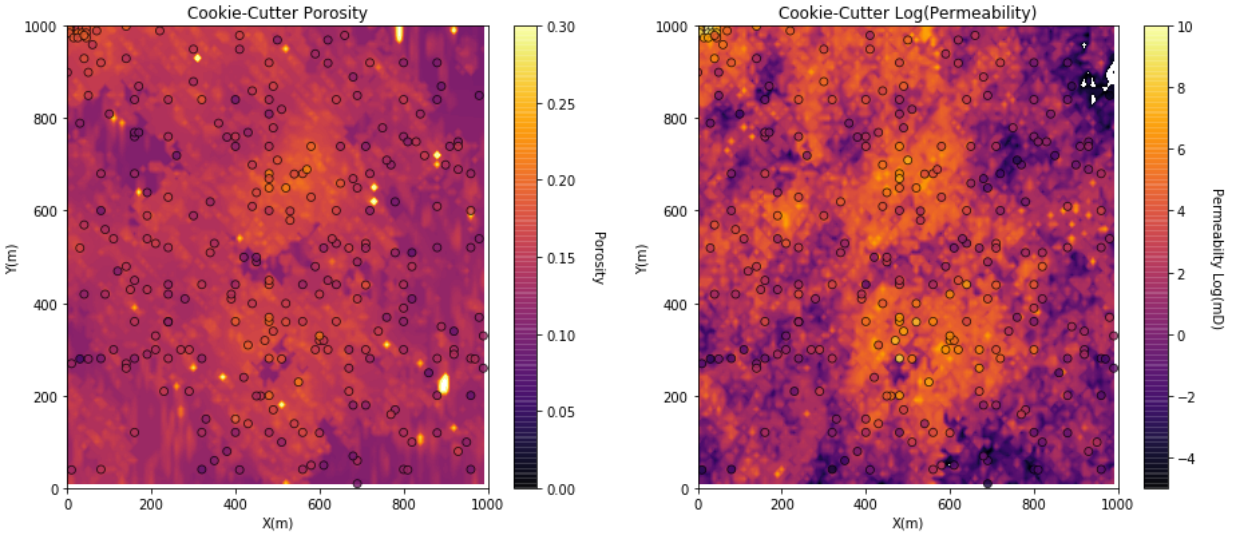

Figure 6: Cookie-cutter plots of one set of simulated data with original well data overlaid (Porosity on left, Permeability on right)

4 Conclusions

Our initial interpretation of the reservoir was that it was a meandering channel. This early interpretation was supported by subsequent work, but after conducting simulations we now have reason to suspect this may be a different depositonal environment. The regions of high permeability resemble lobes (mainly two in the center) in the multiple simulations that have been conducted. We display the acoustic impedance data in Figure 7, to illustrate the consistency with our simulated cookie-cutter models in Figure 6 and actual data collected from the reservoir. However at this point we are now challenging our original interpretation of a meandering channel and suspect that the reservoir might be comprised of lobes instead.

Acoustic Impedance Data

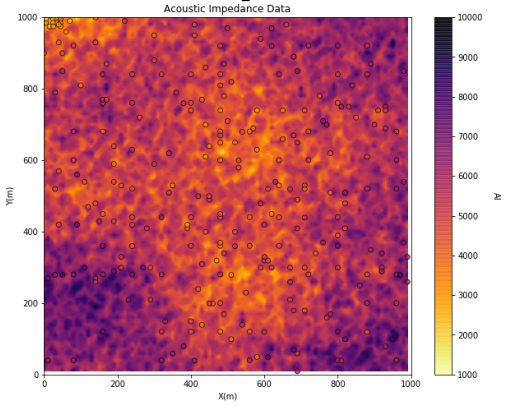

Figure 7: Acoustic Impedance Data